ELSEVIER

Biophysical Chemistry 112 (2004) 117–130

Biophysical Chemistry

www.elsevier.com/locate/bpc

The thrombin–fibrinogen interaction☆

Harold A. Scheraga*

Baker Laboratory of Chemistry, Cornell University, Ithaca, NY 14853-1301, United States

Received 20 April 2004; received in revised form 26 May 2004; accepted 1 July 2004
Available online 17 September 2004

Dedicated to John D. Ferry, a pioneer in the investigation of the thrombin-catalyzed conversion of fibrinogen to fibrin

Abstract

The thrombin-catalyzed conversion of fibrinogen (F) to fibrin consists of three reversible steps, with thrombin (T) being involved in only the first step which is a limited proteolysis to release fibrinopeptides (FpA and FpB) from fibrinogen to produce fibrin monomer. In the second step, fibrin monomers form intermediate polymers through noncovalent interactions. In the third step, the intermediate polymers aggregate to form the fibrin clot. The molecular mechanisms of the first two steps are elucidated.

Keywords: Thrombin; Fibrinogen; Fibrin; Fibrinopeptides; Fibrin clot; Enzymatic hydrolysis; Protein–protein interactions

1. Introduction

A key phase of the blood clotting process is the interaction between thrombin (T) and fibrinogen (F) to form the fibrin clot. It is important that this process be regulated so that clot formation occurs sufficiently rapidly to prevent bleeding from a wound and also so that spontaneous clot formation does not occur when hemostasis is not required.

Blood contains fibrinogen (F) and the precursor of thrombin viz. prothrombin (PT). Both fibrinogen and prothrombin can coexist in circulating blood. However, if blood comes in contact with tissues, as in a wound, prothrombin undergoes a series of enzymatic reactions involving factor VIII, among other species, which lead to thrombin (T) as a smaller protein product. The resulting thrombin can then interact with fibrinogen to form the fibrin clot. One source of hemophilia is a defect in factor VIII which interferes with the ultimate conversion of prothrombin to thrombin and, hence, with the ability to convert fibrinogen to a fibrin clot. This article, dedicated to the memory of John D. Ferry, deals with the mechanism of the interaction of thrombin and fibrinogen to form fibrin.

2. Early observations of Ferry and Morrison

If clear solutions of purified fibrinogen and thrombin are mixed in a test tube, the resulting mixture gradually becomes very opaque. After some time, the tube can be inverted, and its contents will not fall out; that is, a fairly rigid fibrin clot has formed and adheres to the walls of the test tube. Ferry and Morrison [1] made quantitative observations on this reaction, and their results are shown in Fig. 1, where the solid circles represent opacity, and the open circles represent rigidity, of the resulting solution. It can be seen that, after a brief time early in the reaction (indicated by the arrow), there is a rapid rise in the opacity with a concomitant increase in the rigidity of the solution. This critical time, t_c, is referred to as the "clotting time" and occurs much before each of these measured properties has reached its final value.

Fig. 2 shows how t_c depends on pH and ionic strength [2]. At the ionic strength of blood (0.15), clotting is most rapid around pH 7, and the t_c goes to infinity, that is, blood does

☆ This article is based on my John D. Ferry lecture, delivered on May 12, 2003 at the University of Wisconsin.

* Tel.: +1 6072554034; fax: +1 6072544700.
E-mail address: has5@cornell.edu.

0301-4622/$ - see front matter © 2004 Elsevier B.V. All rights reserved.
doi:10.1016/j.bpc.2004.07.011

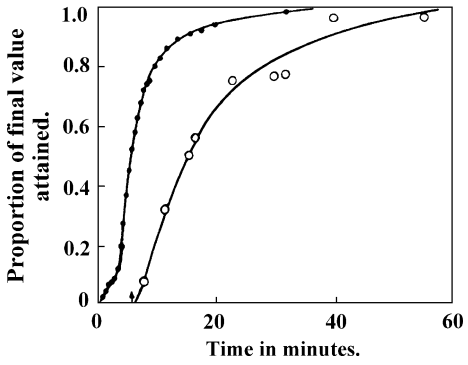

Fig. 1. Rigidity (open circles) and opacity (solid circles), plotted against time, during clotting of a solution with human fibrinogen, concentration 16 g/l, thrombin 1.0 unit/cm^3, ionic strength 0.3, pH 6.33. Arrow denotes clotting time [1].

not clot, as the pH approaches 5 at the low end or above 10 at the high end, with a paraboliclike shape between pH 5 and 10. To interpret the shape of this curve requires an understanding of the mechanism of the interaction between thrombin and fibrinogen, which is the subject of this article.

3. The nature of fibrinogen and thrombin

Fibrinogen, isolated from blood plasma, is a molecule with molecular weight of ~340,000 [3] and has been examined in aqueous solution by hydrodynamic measurements [4–7], such as viscosity, sedimentation velocity, and flow birefringence, by light scattering [5,8–10], by

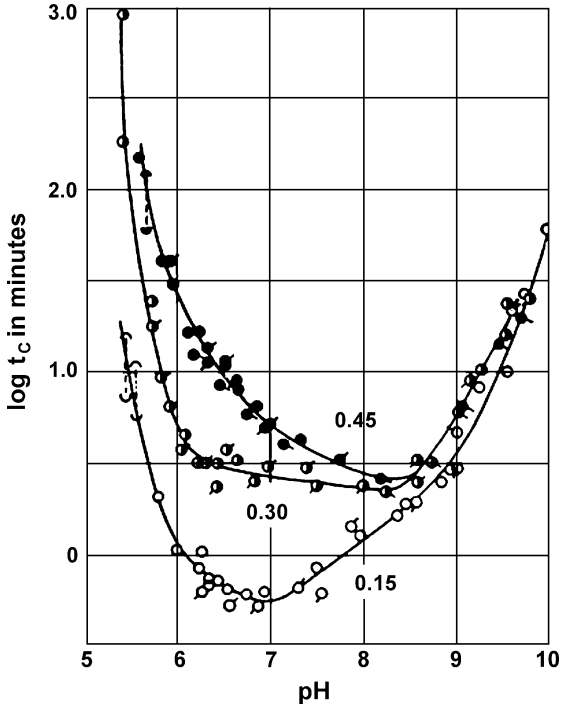

Fig. 2. Logarithm of clotting time plotted against pH for ionic strengths of 0.15, 0.30, and 0.45; bovine fibrinogen concentration 5 g/l, thrombin 1.0 unit/cm^3 [2].

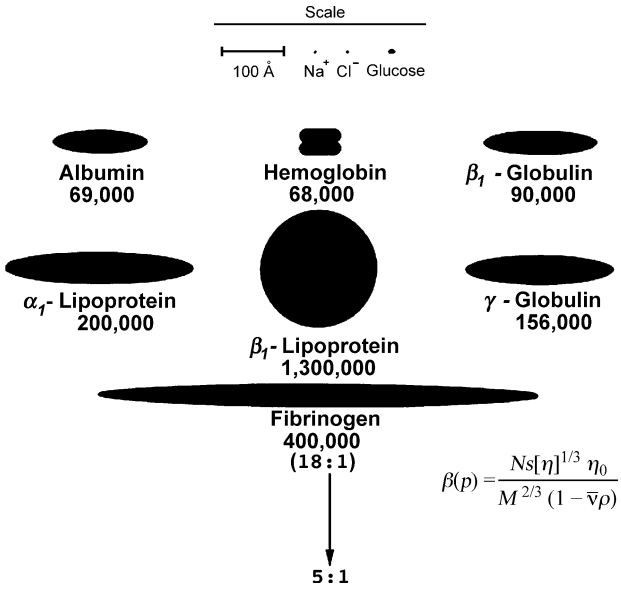

Fig. 3. Early representation of protein molecules in terms of ellipsoids of revolution. Relative dimensions of several protein molecules in blood [19]. The $\beta(p)$ function [18] provided an improved picture of fibrinogen.

electron microscopy [11–13], and by X-ray diffraction [14–17]. The early hydrodynamic and light-scattering observations were interpreted in terms of a prolate ellipsoidal model [18] with a major axis of 450–500 Å and a minor axis of 50–100 Å. This result relied on the use of the $\beta(p)$ function (18, and Fig. 3 [19]) to interpret hydrodynamic data and contrasted with an earlier view of the fibrinogen molecule illustrated in Fig. 3. The molecular dimensions deduced from the $\beta(p)$ function and light scattering are compatible with the electron micrograph shown in Fig. 4; in this micrograph, the overall length of the three-nodule structure is 475±25 Å, the diameters of the outer and middle nodules are 65 and 50 Å, respectively, and the diameter of the links connecting the nodules is <15 Å [11,13]. Biochemical evidence [20–23] suggested that the molecule is a covalently linked dimer, with each half of the dimer

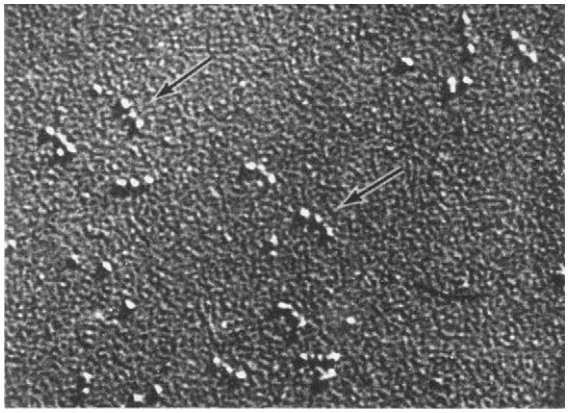

Fig. 4. Electron micrograph of human fibrinogen, showing a three-nodule structure [11].

consisting of three chains, Aα, Bβ, and γ. All six chains of the dimer $(A\alpha, B\beta, \gamma)_2$ are linked by disulfide bonds. Observations by immunoelectron microcopy [24] indicated that the N-termini of the chains (which are also in the DSK fragment of fibrinogen obtained after treatment with cyanogen bromide [25]) are in the central domain (Fig. 5) of the three-nodule structure of Fig. 4 and that the C-termini of the chains are in the symmetrically disposed outer domains (Fig. 6). Recently, this picture has been elucidated by X-ray diffraction studies of human [16] and chicken [17] fibrinogen, as illustrated in Fig. 7. Some functional features of the C-termini of the γ chains [26], determined by enzymatic cleavage studies, are illustrated in Fig. 8; they were subsequently confirmed by X-ray diffraction [15,16], as shown in Fig. 9.

Prothombin is a 582-residue molecule which is proteolitically degraded to the two-chain disulfide-linked thrombin molecule, as illustrated in Fig. 10. Thrombin, with a molecular weight of 39,000, is homologous to trypsin, chymotrypsin, and elastase [27–29]; however, unlike trypsin, which hydrolyzes peptide bonds after arginine and lysine residues, thrombin is much more specific and hydrolyzes specific Arg–Gly bonds near the N-termini of

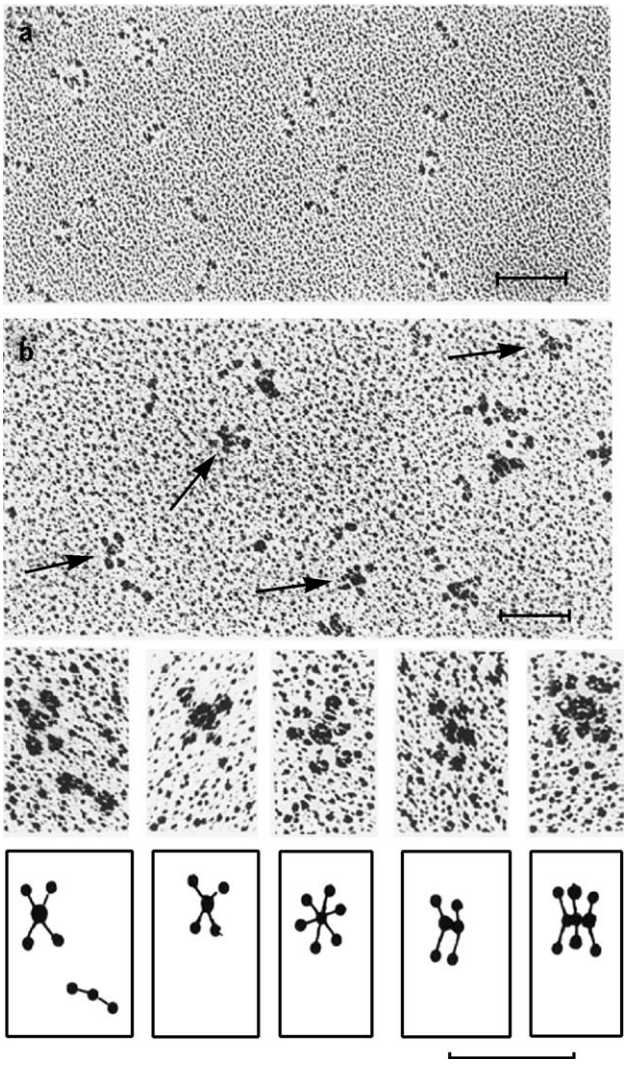

Fig. 5. Electron micrographs (bar=1000Å). (a) Bovine fibrinogen. (b) Complexes of bovine fibrinogen with purified anti-DSK antibodies. Arrows indicate fibrinogen–antibody complexes. (c) Fibrinogen–antibody complexes, with an interpretive drawing given below each frame [24].

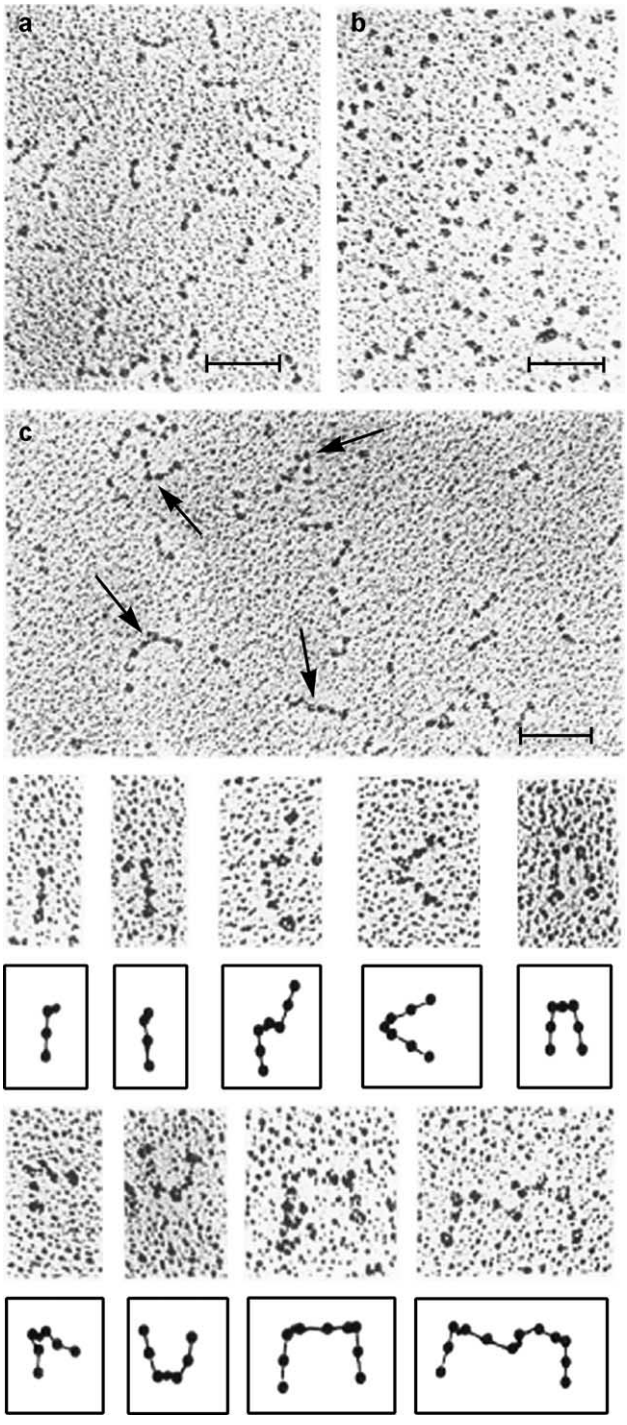

Fig. 6. Electron micrographs (bar=1000Å). (a) Human fibrinogen. (b) Complexes of human fibrinogen with antibodies to a C-terminal peptide from plasmin-digested fibrinogen. Arrows indicate fibrinogen–antibody complexes. (c) Fibrinogen–antibody complexes showing individual fibrinogen molecules with attached antibody, and antibody-linked fibrinogen complexes, with an interpretive drawing given below each frame [24].

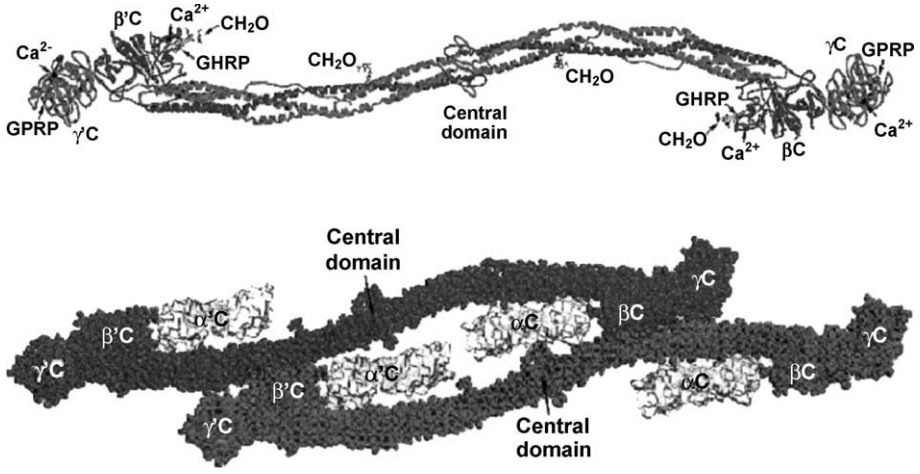

Fig. 7. Top: Ribbon model of the Aα, Bβ and γ chains of chicken fibrinogen showing distal globular domains connected by three-stranded coiled coils that meet at a central focus and other features of the molecule. Bottom: Space filling representation of the ordered parts of two neighboring molecules [14].

the Aα and Bβ chains to produce fibrinopeptides A and B (FpA and FpB), leaving the rest of the chains (α and β) intact [20–23]. Thus, the removal of FpA and FpB uncovers polymerization sites in the α and β chains which react with the C-terminal portions of the γ chains, that are illustrated in Figs. 8 and 9. The X-ray structure of human α-thrombin is shown in Fig. 11 [30].

4. The three-stage reaction

While the overall reaction may be represented as

$$\text{Thrombin(T)} + \text{Fibrinogen(F)} \rightarrow \text{FibrinClot}$$

it has been shown [31,32] that, with *purified* F and T, this reaction consists of three *reversible* steps, namely,

$$\text{F} \underset{\longleftarrow}{\overset{\text{T}}{\longrightarrow}} \text{f} + 2\ \text{FpA} + 2\text{FpB} \tag{1}$$

$$n\text{f} \rightleftarrows \text{f}_n \tag{2}$$

$$m\text{f}_n \rightleftarrows \text{fibrin} \tag{3}$$

where f is fibrin monomer, and n and m are integers. Thrombin is involved only in the enzyme-catalyzed hydrolysis of Step 1.

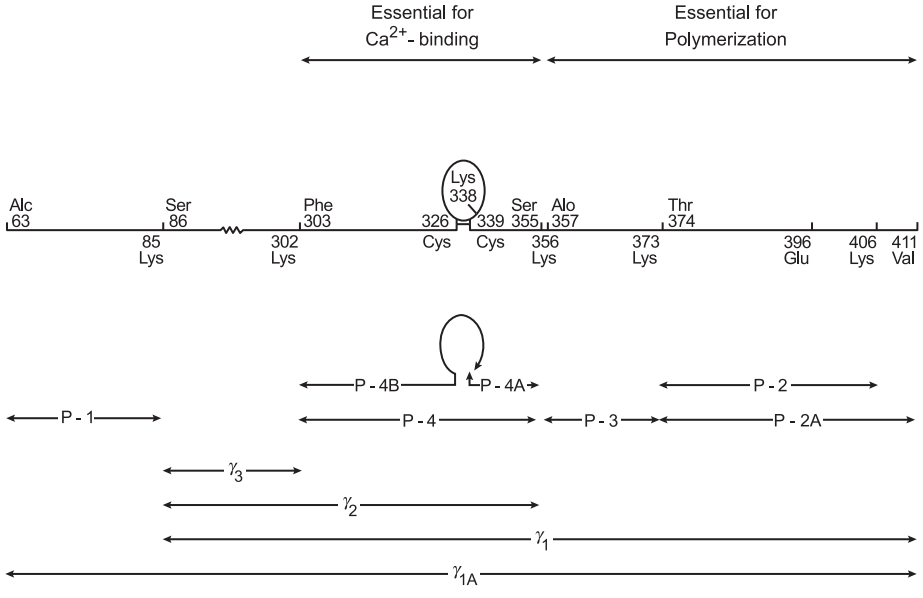

Fig. 8. Schematic representation of the amino acid sequence of the C-terminal portion of the γ chain. The regions essential for polymerization and for Ca^{2+} binding, and the locations of peptides P-1, P-2, P-2A, P-3, and P4 (cleaved by plasmin in the presence of Ca^{2+} or EGTA) are indicated [26].

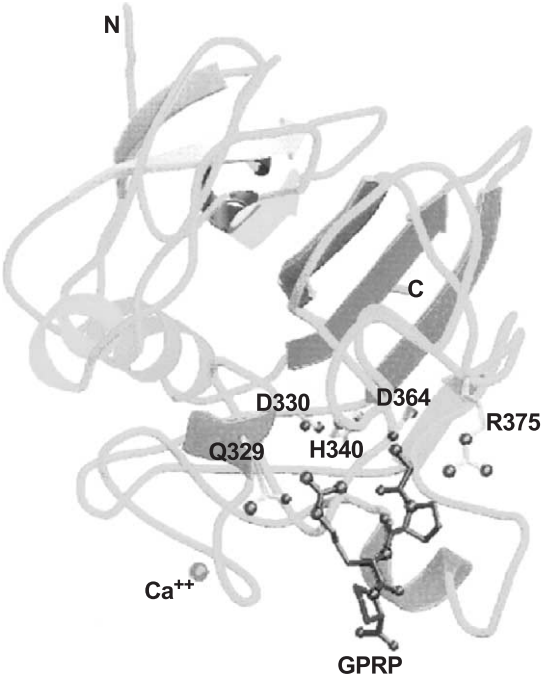

Fig. 9. Model of a 30 kDa C-terminal fragment from the γ chain of human fibrinogen [15].

The reason for the reversibility of Step 1 is illustrated in Fig. 12. Whereas the equilibrium hydrolytic reaction involving, say, a dipeptide is overwhelmingly in the direction of formation of the hydrolytic products, the hydrolysis reaction in Step 1 is reversible, i.e., does not go to completion *in the absence of* Steps 2 *and*3 because the species (F) on the left in Fig. 12 involves noncovalent interactions between FpA (or FpB) and the rest of the fibrinogen molecule, indicated by the dashed lines [33,34]. To liberate FpA or FpB, it would be necessary not only to hydrolyze the peptide bond but also to pay the free energy penalty to disrupt these noncovalent bonds [33].

5. Step 1

The mechanism of action of thrombin on fibrinogen (Step 1) has been investigated by kinetic studies of the hydrolysis of fibrinogen by thrombin in NaBr at pH 5.3 [34,35], where the polymerization of Steps 2 and 3 does not occur, and in KCl at pH 8 before the clotting time [36]; the kinetics of the hydrolysis of fibrinogenlike peptides by thrombin has also been examined [35,37]. Most of these studies have been carried out with peptides based on the N-terminus of the Aα chains of human fibrinogen, with the following amino acid sequence:

$$^{+}\mathrm{H}-\underset{1}{\mathrm{Ala}}-\underset{2}{\mathrm{Asp}}-\underset{3}{\mathrm{Ser}}-\underset{4}{\mathrm{Gly}}-\underset{5}{\mathrm{Glu}}-\underset{6}{\mathrm{Gly}}-\underset{7}{\mathrm{Asp}}-\underset{8}{\mathrm{Phe}}-\underset{9}{\mathrm{Leu}}-\underset{10}{\mathrm{Ala}}-\underset{11}{\mathrm{Glu}}-\underset{12}{\mathrm{Gly}}-\underset{13}{\mathrm{Gly}}-\underset{14}{\mathrm{Gly}}-\underset{15}{\mathrm{Val}}-\underset{16}{\mathrm{Arg}}\downarrow-\underset{17}{\mathrm{Gly}}-\underset{18}{\mathrm{Pro}}-\underset{19}{\mathrm{Arg}}\downarrow-\underset{20}{\mathrm{Val}}-\underset{21}{\mathrm{Val}}-\underset{22}{\mathrm{Glu}}-\underset{23}{\mathrm{Arg}}-\mathrm{OH}^{-}$$

Thrombin hydrolyzes both the Arg16–Gly17 and Arg19–Val20 peptide bonds in *peptides*, but only the Arg16–Gly17 peptide bond in the fibrinogen molecule in which the Arg19–Val20 bond is protected.

Using the Michaelis–Menten scheme

$$E + S \underset{k_b}{\overset{k_f}{\rightleftharpoons}} ES \xrightarrow{k_{cat}} E + P$$

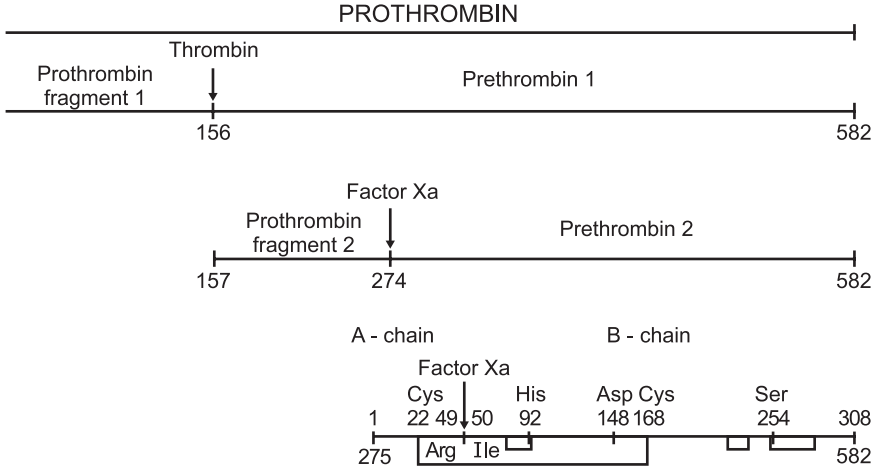

Fig.10. Schematic representation of proteolytic cleavage steps from prothrombin to the disulfide-linked A and B chains of thrombin.

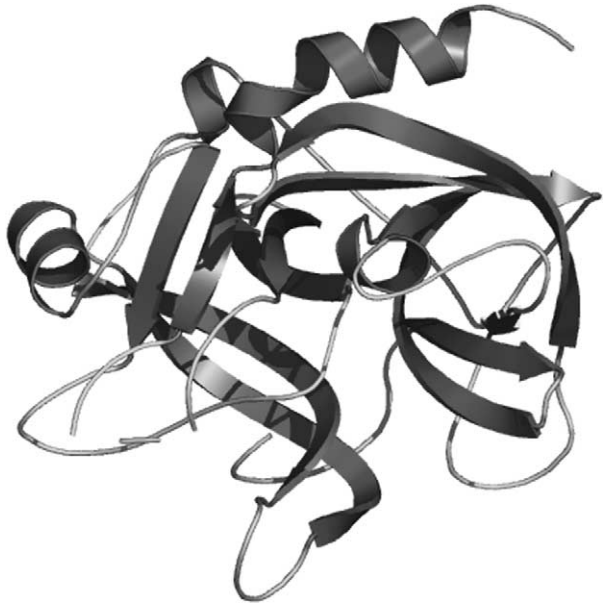

Fig. 11. X-ray crystal structure of human α-thrombin [30].

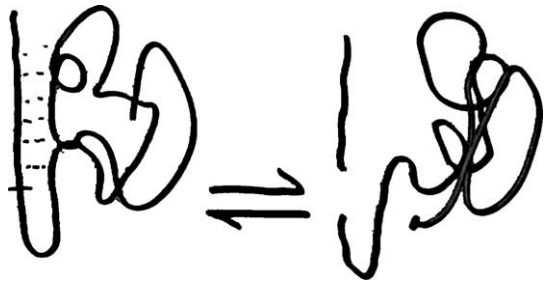

Fig. 12. Schematic illustration of the apparent strengthening of a covalent bond by noncovalent interactions (dashed lines) between a protein and a peptide segment that is to be liberated by proteolysis.

$$\frac{dP}{dt} = \frac{k_{cat}}{K_M}(E)(S)$$

$$K_M = \frac{k_b + k_{cat}}{k_f}$$

the kinetic data are expressed [35] in terms of k_{cat} and K_M (Table 1) with k_{cat}/K_M being a measure of the catalytic efficiency of the enzyme [38]. Although very short peptides are hydrolyzed by thrombin, they are very poor substrates, with values of k_{cat}/K_M being four orders of magnitude smaller than the corresponding value for the Aα chain of intact fibrinogen (or of DSK, a large fibrinogen product obtained after treatment with cyanogen bromide [25]). However, as the chains become longer, especially after the inclusion of Phe8, the value of k_{cat}/K_M approaches that of the intact fibrinogen molecule.

With Phe8 being quite far, in sequence, from the hydrolyzed Arg16–Gly17 peptide bond, it was suggested [35] that this portion of the Aα chain of fibrinogen must be folded to bring Phe8 close to the Arg16–Gly17 sequence. This hypothesis was tested by a transferred NOE NMR experiment [39], whose basis is illustrated in Fig. 13. If two protons, A and B, are far from each other, as indicated at the top of Fig. 13, they do not interact magnetically. When this unfolded peptide binds to, say, a large thrombin molecule, A and B can approach each other in a binding-induced folded structure and can then interact magnetically. When the peptide dissociates from the thrombin, the magnetization state in the folded form relaxes back to that of the unfolded form within a finite time. Given an appropriate relation between this relaxation rate and the on (k_{on}) and off (k_{off}) binding rate constants, it is possible to detect the magnetization state (hence the NOE) of the folded form by measurements on the unfolded

Table 1
Kinetic constants for hydrolysis of Arg–Gly bonds by thrombin (at pH 8.0 and 25°) and conformational equilibrium constants (at pH 8.3 and 4 °C) [35]

Substrate	$k_{cat} \times 10^{11}$ M[(NIH U/L)s]$^{-1}$	$K_M \times 10^6$ M	K_{conf}
1. Aα chain of intact fibrinogen	73	9	Very large
2. Bβ chain of intact fibrinogen	12	11	
3. DSK			4×10^{-3}
4. CNBr Aα	48	47	5×10^{-5}
5. CNBr Bβ	6	189	
6. Ac-Phe-Leu-Ala-Glu-Gly-Gly-Gly-Val-Arg-Gly-Pro-Arg-Val-Val-Arg-$NHCH_3$	11	680	
7. Ac-Leu-Ala-Glu-Gly-Gly-Gly-Val-Arg-Gly-Pro-$NHCH_3$	[a]	[a]	
8. Ac-Ala-Glu-Gly-Gly-Gly-Val-Arg-Gly-Pro-Arg-Val-Val-Glu-Arg-$NHCH_3$	0.3	1560	
9. Ac-Gly-Gly-Val-Arg-Gly-Pro-Arg-Val-Val-Glu-Arg-$NHCH_3$	0.3	630	
10. H-Gly-Gly-Val-Arg-Gly-Pro-Arg-Val-Val-Glu-$NHCH_3$			6×10^{-7}
11. Ac-Phe-Leu-Ala-Glu-Gly-Gly-Gly-Val-Arg-Gly-Pro-Arg-Val-Val-Glu-$NHCH_3$	16	789	
12. H-Phe-Leu-Ala-Glu-Gly-Gly-Gly-Val-Arg-Gly-Pro-Arg-Val-Val-Glu-$NHCH_3$			11×10^{-7}
13. Ac-Phe-Leu-Ala-Glu-Gly-Gly-Gly-Val-Arg-Gly-Pro-Arg-Val-$NHCH_3$	20	633	
14. Ac-Phe-Leu-Ala-Glu-Gly-Gly-Gly-Val-Arg-Gly-Pro-$NHCH_3$	11	934	
15. H-Gly-Val-Arg-Gly-Pro-Arg-Leu-OH	0.5	3700	
16. H-Gly-Val-Arg-Gly-Gly-Arg-Leu-OH	0.2	9600	
17. H-Gly-Val-Arg-Gly-Pro-Gly-Leu-OH	0.1	15300	

[a] While the values of k_{cat} and K_M could not be determined, this peptide is hydrolyzed by thrombin much more slowly than peptide 14.

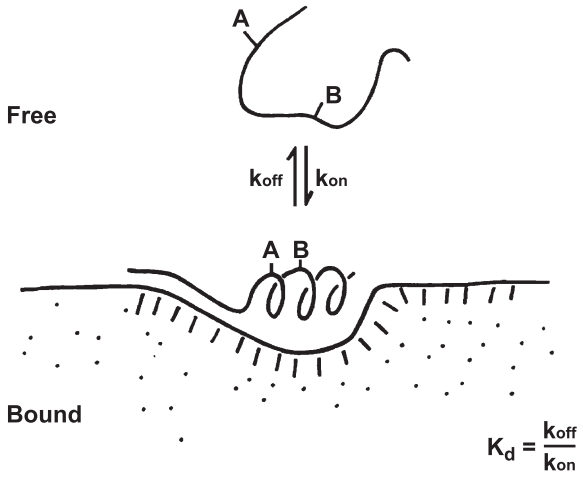

Fig. 13. Schematic illustration of the interaction of thrombin with peptides derived from proteins such as fibrinogen and hirudin. The peptides in solution can assume an ensemble of conformations. Protons A and B are, on average, far away in the free peptide; however, in the bound state, they may be nearby in space. The proximity between protons A and B in the bound state can be established by transferred NOE experiments [39].

form because the thrombin molecule is too large compared to the peptide to affect the NOE signal from the folded peptide. From such transferred NOEs, it is possible to compute the distances between pairs of protons and thereby deduce the structure of the peptide in the bound, folded form. Fig. 14 illustrates the NOEs that were detected in such an experiment [40], and Fig. 15 illustrates the structure that was deduced [40], from these NOEs. It can be seen that Phe8 is close to Arg16 in the folded form. Presumably, this portion of the Aα chain of fibrinogen has the same three-dimensional structure as deduced for the peptide by the transferred NOE experiment. Unfortunately, FpA and FpB could not be resolved in the X-ray structure of fibrinogen [17]. If thrombin is inactivated by covalently blocking the active site to form PPACK thrombin (where PPACK is D-Phe–Pro arginine chloromethyl ketone), these fibrinogenlike peptides do not bind, and no transferred NOEs can be detected.

There are many bleeding disorders manifested by low clottability arising from genetic mutations in the FpA portion of fibrinogen [41]. In one of these (Fibrinogen Rouen), Gly12 is replaced by Val12 [41]. The bottom part of Fig. 16 is the computer generated structure of Fig. 15, but with Val12 substituted for Gly12. From knowledge of the Ramachandran diagrams for Val and Gly, it is clear that valine cannot occupy position 12 that is occupied by glycine in Fig. 15. The structure at the top of Fig. 16 is the one determined by a transferred NOE experiment on a peptide containing valine instead of glycine at position 12 [42]. The altered structure presumably prevents the Arg–Gly bond from being properly oriented in the active site pocket of thrombin, thereby preventing its hydrolysis. This constitutes a structural interpretation for the origin of a bleeding disorder.

A common inhibitor of thrombin is the 65-residue protein, hirudin [43]. The three-dimensional structure of hirudin has been determined by NMR spectroscopy by Sukumaran et al. [44] and by Haruyama and Wüthrich [45]; however, because of nonregular, unfolded structure at the C-terminus, the structure of this portion of the hirudin molecule could not be determined. However, the C-terminal portion (shown below) contains the binding site for thrombin [46]. Presumably, the C-terminal portion of hirudin adopts a unique structure when it is bound to thrombin.

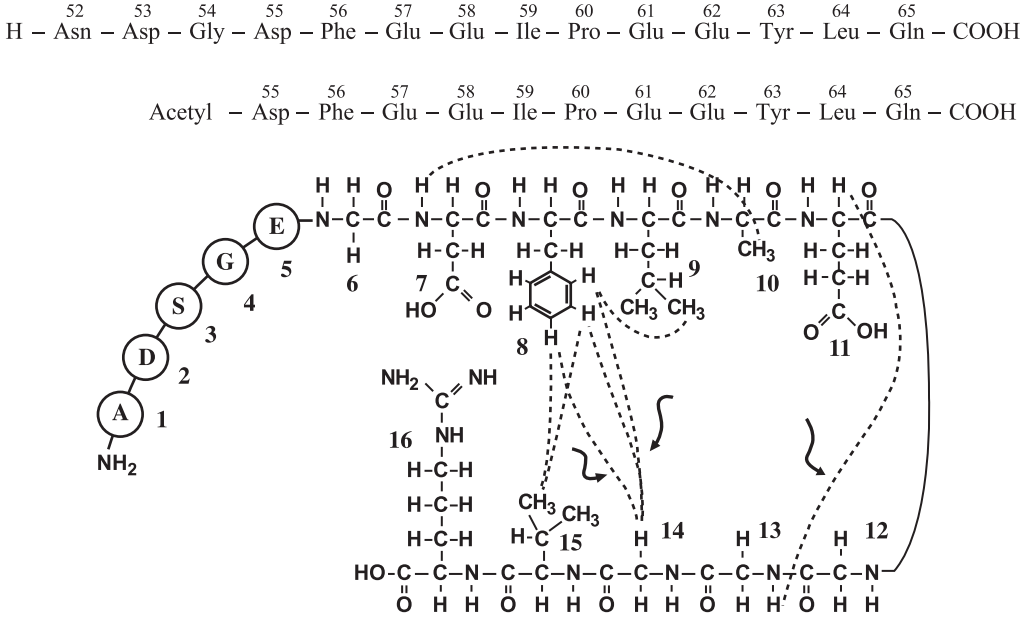

Fig. 14. Proximity relations of protons of FpA in the thrombin-bound state. The circled residues are those whose proton resonances were not affected by thrombin binding. The arrows indicate the NOEs that are absent when Gly12 is replaced by Val12 in FpA [39].

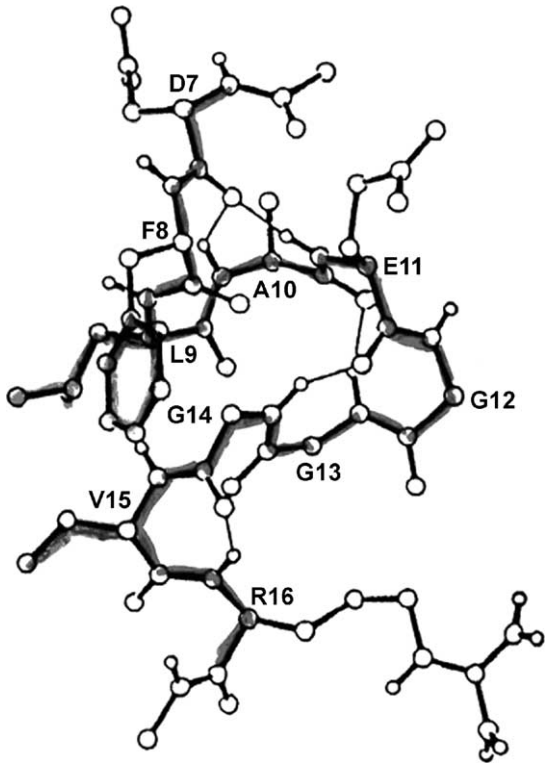

Fig. 15. Proposed structure of thrombin-bound FpA. A thin line connecting an oxygen atom to a hydrogen atom indicates that those two atoms are separated by less than 2.0 Å (hydrogen bonds). The nonpolar cluster formed by the side chains of Phe8, Leu9, and Val15 is clearly seen [40].

The same transferred NOE technique was applied to complexes of each of these peptides with thrombin [47]. Fig. 17 illustrates the observed NOEs, and Fig. 18 shows the computed three-dimensional structure of the C-terminus of hirudin, based on these NOEs [39,47]. An X-ray structure of a complex of the whole hirudin molecule with thrombin, in which the C-terminus of hirudin was immobilized [48], led to a structure of hirudin in which the structure of the C-terminus was comparable to that deduced from the transferred NOE experiment, as shown in Table 2.

Although the active (primary) site of thrombin is blocked by PPACK, the above hirudin peptides bind to *both* thrombin and PPACK thrombin with identical transferred NOEs [47]. This is because there is a secondary binding site on thrombin [49], separate from the primary one that binds FpA and FpB, to which these hirudin peptides bind. The inhibitory action of the *whole* hirudin molecule presumably arises when the C-terminus of hirudin binds to the secondary binding site of thrombin while the rest of the hirudin molecule occludes the primary site of thrombin [15,48,50]. An X-ray structure of a complex between thrombin and the central domain of fibrin, which is devoid of FpA and FpB, localized the secondary binding site [51].

6. Step 2

It is possible to investigate Step 2 in the absence of thrombin by preparing purified fibrin monomer, f, by dissolving fibrin (because of the reversibility of Steps 2 and 3) and maintaining the solution at pH 5 [52], where, as shown in Fig. 2, f does not polymerize. Then, as the pH is raised to a value between 5 and 10, polymerization occurs. By limiting the observations to the early part of the reaction, before Step 3 can occur, it is possible to examine the mechanism of Step 2.

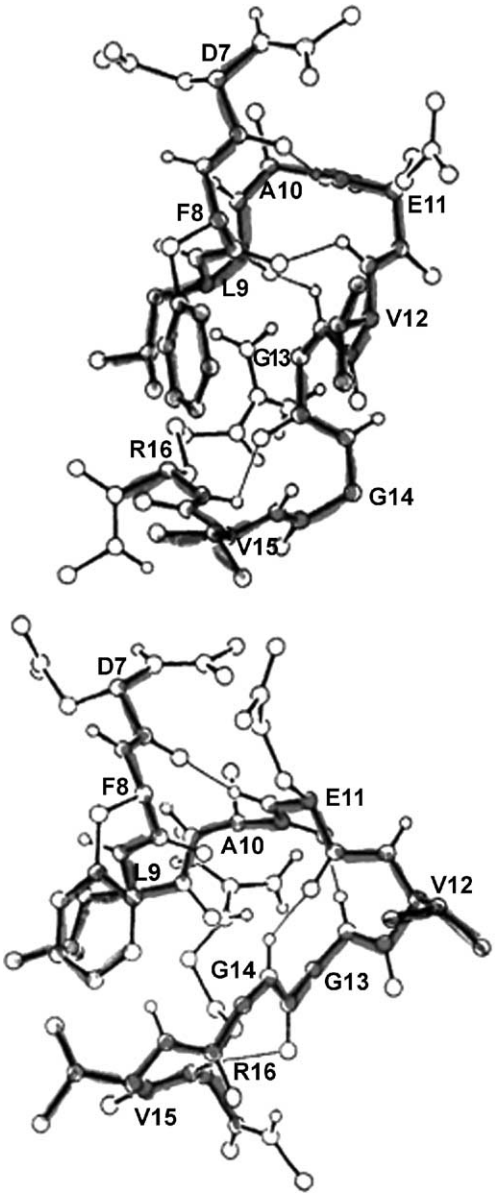

Fig. 16. Top: Proposed structure of the Val12 variant of FpA in the thrombin-bound state. Bottom: A hypothetical structure of this peptide constructed from the model of Fig. 15 by replacing Gly12 with Val12. A thin line connecting an oxygen atom to a hydrogen atom indicates that those two atoms are separated by less than 2.0 Å (hydrogen bonds) [39].

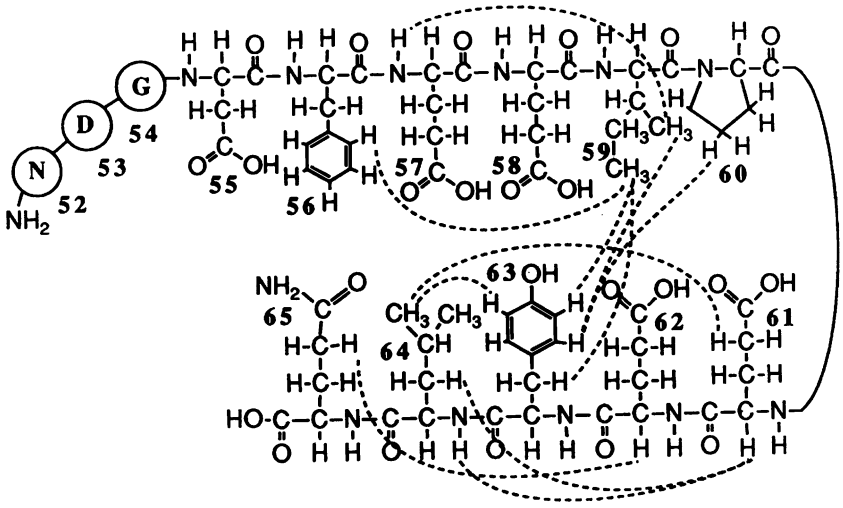

Fig. 17. Proximity relations of protons of residues 52–65 of the hirudin C-terminus in the thrombin-bound state. The circled residues are those whose proton resonances were not affected by thrombin binding [39].

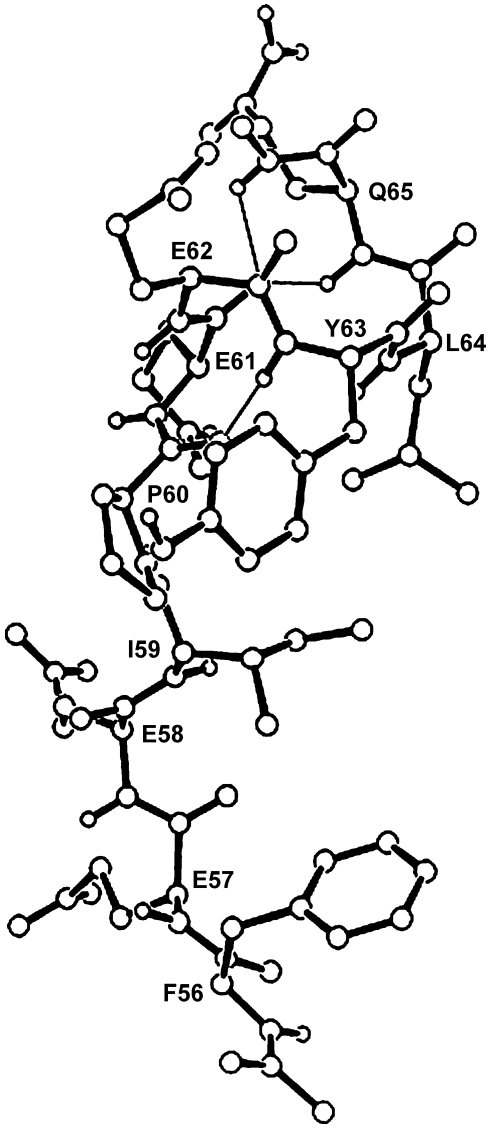

Fig. 18. A model structure of residues Phe56 to Gln65 of the hirudin C-terminus on the basis of NOE-constrained molecular modeling [39,47].

Fig. 19, based on flow birefringence measurements [6,7], shows that whereas the length of the fibrin-monomer molecule is ~500Å, similar to that of fibrinogen at the extremes of the pH range, the lengths of the intermediate polymers that form early in the reaction at neutral pH appear to be over 10 times the length of the monomer. Interestingly, the "parabolic" shape of the curve of Fig. 19 resembles that of Fig. 2—that is, the pH dependence of t_c resembles the pH dependence of Step 2—a point to which we shall return below (Fig. 2 reflects the pH dependence of Step 2, superimposed on that of Step 1). Based on these and other hydrodynamic measurements [4–7], the model of Fig. 20 was proposed [35,53,54] as the structure of the intermediate polymers, in which there is a staggered overlap of two chains of f_n (with variable n).

The models of F, f, and the intermediate polymers f_n of f, deduced from hydrodynamic and light-scattering measurements, which also provided information about the distribution of the sizes, n, of f_n [52], were confirmed by electron microscopy [54]. Fig. 21a and b illustrates the familiar, three-nodule structure of F and f, respectively (cf. Fig. 4). Fig. 22a shows the staggered-overlap feature of a dimer and a longer polymer, and Fig. 22b shows a staggered–overlapping

Table 2
Comparison of NMR structure of hirudin fragment (with bovine thrombin) with X-ray structure of whole hirudin molecule (with human thrombin)

Residue	Cα RMSD (Å)	
56 Phe	5.75	52 Asn and 53
57 Glu	0.93	ASP are not bound
58 Glu	0.91	
59 Ile	0.58	
60 Pro	0.28	
61 Glu	0.40	
62 Glu	0.28	
63 Tyr	0.38	
64 Leu	1.08	
65 Gln	1.45	

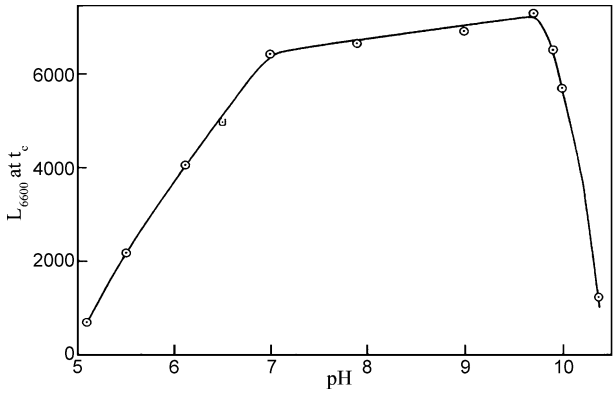

Fig. 19. Dependence of length (in Å at the clotting time) on pH at a velocity gradient of 6600 sec^{-1}[6,7].

tetramer. Several staggered-overlapping trimers are shown in Fig. 23, and a very elongated staggered-overlapping intermediate polymer is shown in Fig. 24. The overlapping presumably arises when preexisting polymerization sites in the C-terminal portion of the γ-chain (Figs. 8 and 9) contact the polymerization sites that are formed at the N-termini of the α and β chains by liberation of FpA and FpB by thrombin (Figs. 5 and 6).

In order to identify the nature of the contacts between the polymerization sites at the N- and C-termini, it is necessary to explain three observations:

(1) Polymerization occurs only in the pH range between 5 and 10 (Figs. 2 and 19).
(2) Pure fibrin can be dissolved at increased temperature (above ~42 °C) at pH 5 to form fibrin monomer [52]; this is the reverse of the exothermic reactions ($\Delta H<0$) for the polymerization of f.
(3) Polymerization of f leads to a liberation of protons between pH 5 and 7.5, and an uptake of protons between pH 7.5 and 10 [55,56].

Clearly, because of point 2, the ease of reversing polymerization by heating, the interactions must be non-covalent, i.e., involving hydrogen and/or hydrophobic bonds. However, since $\Delta H<0$, the interactions must be

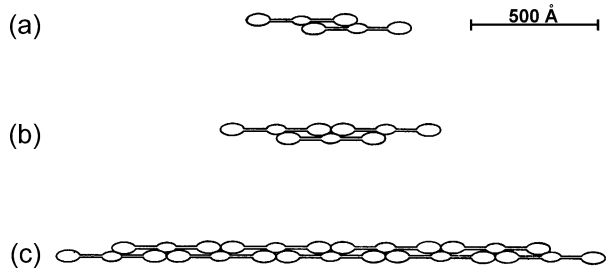

Fig. 20. Schematic illustration of staggered overlap of intermediate polymers. (a) Dimer, (b) trimer, (c) longer intermediate polymer. Note how the central nodule of one monomer contacts the outer nodules of two other (adjacent) monomers [35].

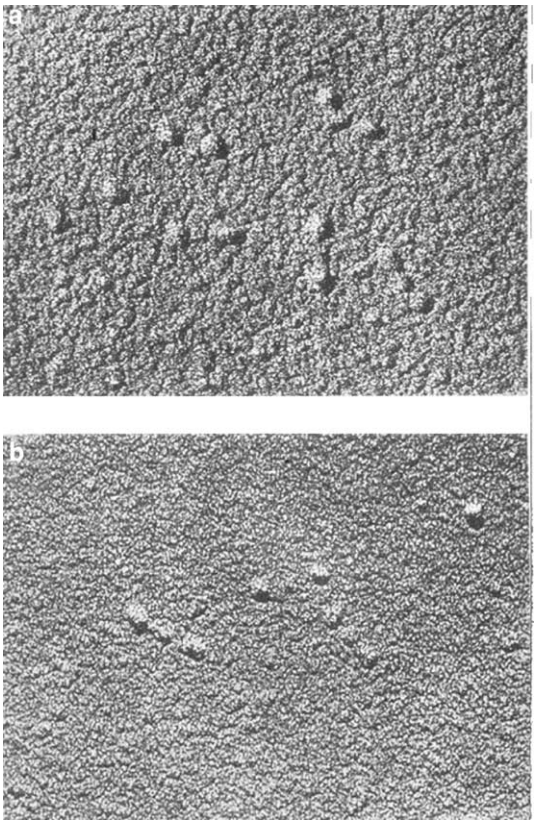

Fig. 21. Electron micrograph of (a) bovine fibrinogen and (b) fibrin monomer [54].

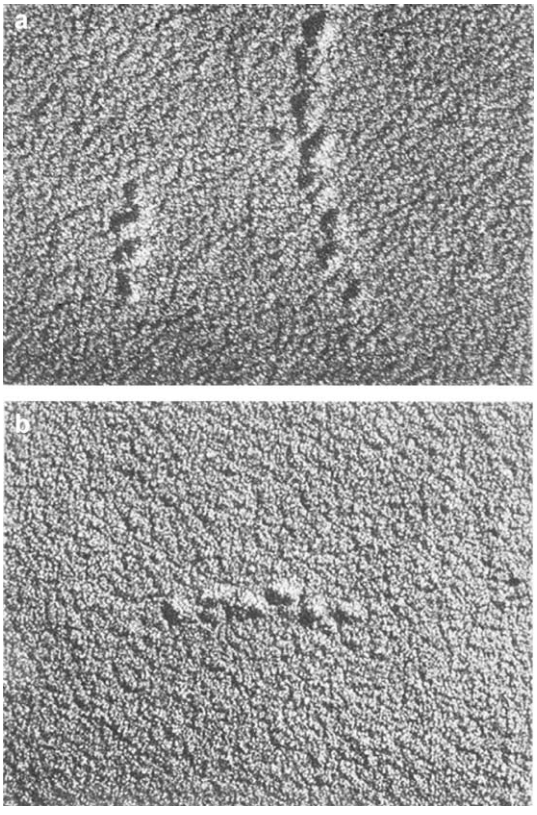

Fig. 22. Electron micrograph of (a) fibrin dimer (left) and part of a higher intermediate polymer (right); (b) fibrin tetramer [54].

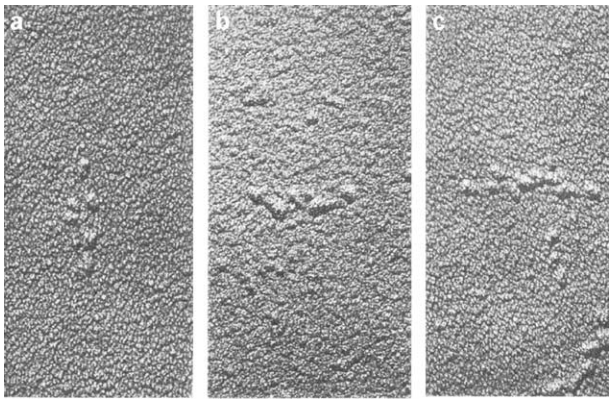

Fig. 23. Electron micrographs of several images of fibrin trimers [54].

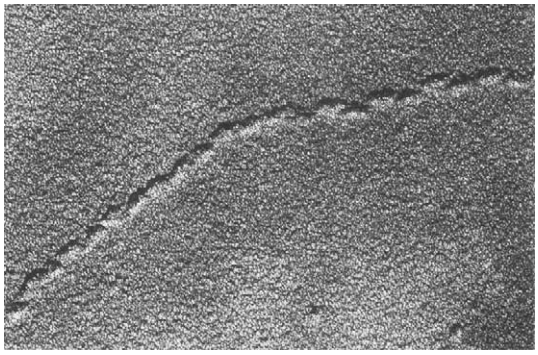

Fig. 24. Electron micrograph of part of a high intermediate fibrin polymer [54].

overwhelmingly hydrogen rather than hydrophobic bonds. The polymerization process can thus be represented [55] as

$$\mathrm{DH} + \mathrm{A} \underset{}{\overset{K_1}{\rightleftharpoons}} \mathrm{DH}\cdots\mathrm{A}$$

where DH is a hydrogen bond donor, and A is a hydrogen bond acceptor. If these are themselves ionizable groups,

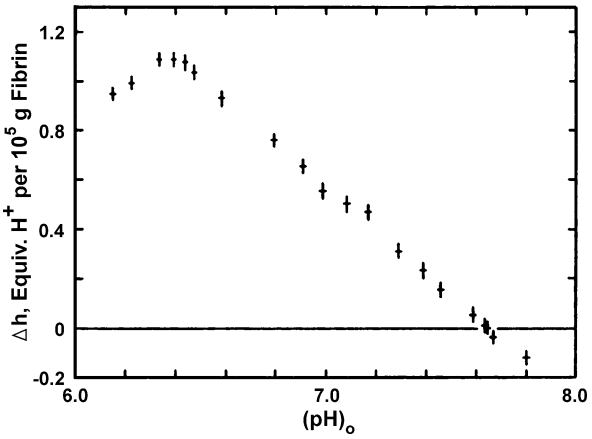

Fig. 26. Proton release or absorption in the polymerization of fibrin in 1.0 M NaBr, 25.0°, as a function of initial pH [56].

then the following two additional equilibria must also be involved:

$$\mathrm{DH} \underset{}{\overset{K_2}{\rightleftharpoons}} \mathrm{H}^+ + \mathrm{D}^-$$

and

$$\mathrm{AH}^+ \underset{}{\overset{K_3}{\rightleftharpoons}} \mathrm{H}^+ + \mathrm{A}.$$

Solution of the above three simultaneous equilibria provides the pH dependence of the number of protons liberated (q in Fig. 25) and, with the heats of ionization of DH and AH^+, the pH dependence of the overall ΔH for the polymerization reaction [55]. Computations with assumed values of K_1, K_2, and K_3, and their corresponding ΔH values lead to the curves shown in Fig. 25. The asymmetry of the ΔH curve arises because the ΔH values for ionization of DH and AH^+ were assumed to differ. The position of the maximum in the q vs. pH curve provides the pK_a of the acceptor group, and the position of the minimum provides the pK_a of the donor group. The crossing-point pH at q=0

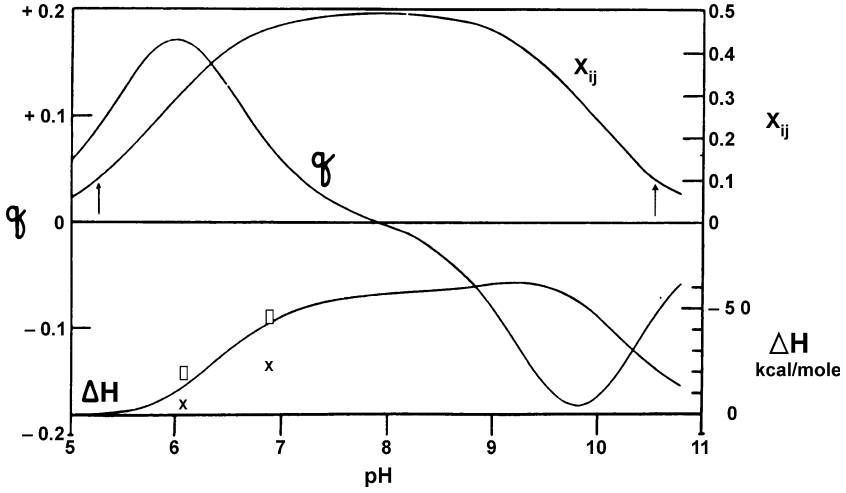

Fig. 25. Curves showing pH dependence of x_{ij}, q, and ΔH for Step 2, computed from hypothetical values of K_1, K_2 and K_3. The experimental points at pH 6.08 and 6.88, indicated by the rectangles, are included for comparison with the theoretical curve. The crosses are theoretical points obtained for an alternative value of K_1 [55].

depends on the pK_a values of both the donor and the acceptor. At a pH, say, around 6, the donor group, with a high pK_a is unaffected by the DH+A polymerization reaction. However, at pH 6, the DH+A reaction (with a pK_a near 6 for AH^+) removes A from its ionization equilibrium with AH^+. Hence, this equilibrium is shifted to the right, producing protons, as illustrated in Fig. 25. At a higher pH, say, around 10, all of the AH^+ groups are in the dissociated form A and are unaffected by the DH+A polymerization. However, at pH 10, the DH+A reaction (with a pK_a near 10 for DH) removes DH from its ionization equilibrium with D^-. Hence, this equilibrium is shifted to the left, with an uptake of protons, as illustrated in Fig. 25. Experimental data, obtained by raising the pH of fibrin monomer solutions from 5 to higher values [56], are shown in Fig. 26. From the position of the maximum, it is concluded that the pK_a of AH^+ is ~6; that is, that the acceptor A is a histidine from which the proton has dissociated. The curve in Fig. 26 resembles part of the q vs. pH curve of Fig. 25. Because of instability of the electrodes at high pH, it was not possible to obtain the experimental high pH portion of the q vs. pH curve. However, since the experimental crossing-point pH, which is the average of the pK values of AH^+ and DH, was obtainable, it was deduced that the pK_a of DH is ~10; that is, that the donor DH is a tyrosine with its proton intact.

This model accounts for the pH range of polymerization (see the x_{ij} curve of Fig. 25, where x_{ij} is the fraction of the molecules in the DH···A form at any pH), and for the pH-dependent ΔH of ionization, shown as two experimental points [55] on the ΔH vs. pH curve of Fig. 25. Further details about the mechanism of polymerization of fibrin monomer were provided by Endres and Scheraga [57].

It is worth noting that the negative ΔH, arising from the hydrogen bond mechanism, is almost unique in the protein literature. Most other protein–protein interactions are endothermic, involving the predominance of hydrophobic interactions [58–60]. Hydrophobic interactions could also be involved in the DH+A polymerization step, but would not be observable because they do not involve ionizable groups. However, as shown by Némethy et al. [61] and by Fernández and Scheraga [62] (see Fig. 1 of each paper), hydrophobic groups can increase the strength of hydrogen bonds by interacting with the nonpolar "necks" of side chains such as glutamic acid or lysine.

Two related experiments support the conclusion that tyrosyl...histidine hydrogen bonds are involved in the polymerization of Step 2. First, photooxidation of histidine leads to loss of polymerization [63]. Second, iodinated fibrinogen, in which the tyrosines are in the form of di-iodotryosine with a pK_a of ~7, exhibits the same polymerization behavior as native fibrinogen, except for a shift in properties [64], consistent with a shift in pK_a of DH from 10 to 7.

Our laboratory has not produced any mechanistic observations on Step 3, other than to demonstrate its reversibility. Further details about the mechanisms of Steps 1 and 2 are provided in Refs. [32–35] and [57].

7. Conclusions

While the observations of Fig. 2 presented a challenge for obtaining a molecular mechanistic interpretation, it appears that the reversible three-step model, based on various physical–chemical observations, provides such an interpretation. In addition, the thrombin–fibrinogen interaction has been the vehicle for developing several concepts of protein chemistry dealing with the reversibility of enzymatic hydrolysis and of protein–protein interactions.

References

[1] J.D. Ferry, P.R. Morrison, Preparation and properties of serum and plasma proteins: VIII. The conversion of human fibrinogen to fibrin under various conditions, J. Am. Chem. Soc. 69 (1947) 388–400.
[2] S. Shulman, J.D. Ferry, The conversion of fibrinogen to fibrin: II. Influence of pH and ionic strength on clotting time and clot opacity, J. Phys. Colloid Chem. 54 (1950) 66–79.
[3] H.A. Scheraga, W.R. Carroll, L.F. Nims, E. Sutton, J.K. Backus, J.M. Saunders, Hydrodynamic properties of urea-denatured fibrinogen, J. Polym. Sci. 14 (1954) 427–442.
[4] S. Shulman, J.D. Ferry, The conversion of fibrinogen to fibrin: III. Sedimentation and viscosity studies on clotting systems inhibited by hexamethylene glycol, J. Phys. Colloid Chem. 55 (1951) 135–144.
[5] C.S. Hocking, M. Laskowski Jr., H.A. Scheraga, Size and shape of bovine fibrinogen, J. Am. Chem. Soc. 74 (1952) 775–778.
[6] H.A. Scheraga, J.K. Backus, Flow birefringence in arrested clotting systems, J. Am. Chem. Soc. 74 (1952) 1979–1983.
[7] J.K. Backus, M. Laskowski Jr., H.A. Scheraga, L.F. Nims, Distribution of intermediate polymers in the fibrinogen–fibrin conversion, Arch. Biochem. Biophys. 41 (1952) 354–366.
[8] R.F. Steiner, K. Laki, Light-scattering studies on fibrinogen: preliminary remarks, J. Am. Chem. Soc. 73 (1951) 882–883.
[9] R.F. Steiner, K. Laki, Light-scattering studies on the clotting of fibrinogen, Arch. Biochem. Biophys. 34 (1951) 24–37.
[10] S. Katz, K. Gutfreund, S. Shulman, J.D. Ferry, The conversion of fibrinogen to fibrin: X. Light scattering studies of bovine fibrinogen, J. Am. Chem. Soc. 74 (1952) 5706–5709.
[11] C.E. Hall, Electron microscopy of fibrinogen and fibrin, J. Biol. Chem. 179 (1949) 857–864.
[12] B.M. Siegel, J.P. Mernan, H.A. Scheraga, The configuration of native and partially polymerized fibrinogen, Biochim. Biophys. Acta 11 (1953) 329–336.
[13] H.S. Slayter, Electron microscopic studies of fibrinogen structure: historical perspectives and recent experiments, Ann. N.Y. Acad. Sci. 408 (1983) 131–145.
[14] V.C. Yee, K.P. Pratt, H.C.F. Côté, I. Le Trong, D.W. Chung, E.W. Davie, R.E. Stenkamp, D.C. Teller, Crystal structure of a 30 kDa C-terminal fragment from the γ chain of human fibrinogen, Structure 5 (1997) 125–138.
[15] K.P. Pratt, H.C.F. Côté, D.W. Chung, R.E. Stenkamp, E.W. Davie, The primary fibrin polymerization pocket: three-dimensional structure of a 30-kDa C-terminal γ chain fragment complexed with the peptide Gly–Pro–Arg–Pro, Proc. Natl. Acad. Sci. U. S. A. 94 (1997) 7176–7181.
[16] H.C.F. Côté, K.P. Pratt, E.W. Davie, D.W. Chung, The polymerization pocket "a" within the carboxyl-terminal region of the γ chain of

human fibrinogen is adjacent to but independent from the calcium-binding site, J. Biol. Chem. 272 (1997) 23792–23798.
[17] Z. Yang, J.M. Kollman, L. Pandi, R.F. Doolittle, Crystal structure of native chicken fibrinogen at 2.7 Å resolution, Biochemistry 40 (2001) 12515–12523.
[18] H.A. Scheraga, L. Mandelkern, Consideration of the hydrodynamic properties of proteins, J. Am. Chem. Soc. 75 (1953) 179–184.
[19] G. Scatchard, Molecular interactions in protein solutions, Am. Sci. 40 (1952) 61–83.
[20] L. Lorand, Fibrino-peptide: new aspects of the fibrinogen–fibrin transformation, Nature 167 (1951) 992–993.
[21] L. Lorand, Fibrino-peptide, Biochem. J. 52 (1952) 200–203.
[22] F.R. Bettelheim, K. Bailey, The products of the action of thrombin on fibrinogen, Biochim. Biophys. Acta 9 (1952) 578–579.
[23] B. Blombäck, I. Yamashina, Determination of N-terminal amino acids during the conversion of fibrinogen to fibrin, Acta Chem. Scand. 11 (1957) 194–195.
[24] J.N. Telford, J.A. Nagy, P.A. Hatcher, H.A. Scheraga, Location of peptide fragments in the fibrinogen molecule by immunoelectron microscopy, Proc. Natl. Acad. Sci., U. S. A. 77 (1980) 2372–2376.
[25] B. Blombäck, B. Hessel, S. Iwanaga, J. Reuterby, M. Blombäck, Primary structure of human fibrinogen and fibrin: I. Cleavage of fibrinogen with cyanogen bromide. Isolation and characterization of NH_2-terminal fragments of the α ("A") chain, J. Biol. Chem. 247 (1972) 1496–1512.
[26] A. Váradi, H.A. Scheraga, Localization of segments essential for polymerization and for calcium binding in the γ-chain of human fibrinogen, Biochemistry 25 (1986) 519–528.
[27] B.S. Hartley, Homologies in serine proteinases, Philos. Trans. R. Soc. Lond., B 257 (1970) 77–87.
[28] S. Magnusson, Thrombin and prothrombin, 3rd edit.P.D. Boyer (Ed.), The Enzymes, vol. 3, Academic Press, New York, NY, 1971, pp. 277–321.
[29] S. Magnusson, T.E. Petersen, L. Sottrup-Jensen, H. Claeys, Complete primary structure of prothrombin: isolation, structure and reactivity of ten carboxylated glutamic acid residues and regulation of prothrombin activation by thrombin, in: E. Reich, D.B. Rifkin, E. Shaw (Eds.), Proteases and Biological Control, Cold Spring Harbor Laboratory, Cold Spring, N.Y., 1975, pp. 123–149.
[30] W. Bode, I. Mayr, U. Baumann, R. Huber, S.R. Stone, J. Hofsteenge, The refined 1.9Å crystal structure of human α-thrombin: interaction with D-Phe–Pro–Arg chloromethylketone and significance of the Tyr–Pro–Pro–Trp insertion segment, EMBO J. 8 (1989) 3467–3475.
[31] M. Laskowski Jr., D.H. Rakowitz, H.A. Scheraga, Equilibria in the fibrinogen–fibrin conversion, J. Am. Chem. Soc. 74 (1952) 280.
[32] H.A. Scheraga, M. Laskowski Jr., The fibrinogen–fibrin conversion, Adv. Protein Chem. 12 (1957) 1–131.
[33] M. Laskowski Jr., H.A. Scheraga, Thermodynamic considerations of protein reactions: II. Modified reactivity of primary valence bonds, J. Am. Chem. Soc. 78 (1956) 5793–5798.
[34] M. Laskowski Jr., T.H. Donnelly, B.A. Van Tijn, H.A. Scheraga, The proteolytic action of thrombin on fibrinogen, J. Biol. Chem. 222 (1956) 815–821.
[35] H.A. Scheraga, Interaction of thrombin and fibrinogen and the polymerization of fibrin monomer, Ann. N.Y. Acad. Sci. 408 (1983) 330–343.
[36] H.A. Scheraga, Active site mapping of thrombin, in: R.L. Lundblad, J.W. Fenton II, K.G. Mann (Eds.), Chemistry and Biology of Thrombin, Ann Arbor Science Publishers, Ann Arbor, MI, 1977, pp. 145–158.
[37] L.S. Hanna, H.A. Scheraga, C.W. Francis, V.J. Marder, Comparison of structures of various human fibrinogens and a derivative thereof by a study of the kinetics of release of fibrinopeptides, Biochemistry 23 (1984) 4681–4687.
[38] I. Schechter, A. Berger, On the size of the active site in proteases: I. Papain, Biochem. Biophys. Res. Commun. 27 (1967) 157–162.
[39] F. Ni, K.D. Gibson, H.A. Scheraga, Nuclear magnetic resonance studies of thrombin–fibrinopeptide and thrombin–hirudin complexes, in: L.J. Berliner (Ed.), Thrombin Structure and Function, Plenum Press, New York, 1992, pp. 63–85.
[40] F. Ni, Y.C. Meinwald, M. Vásquez, H.A. Scheraga, High-resolution NMR studies of fibrinogen-like peptides in solution: structure of a thrombin-bound peptide corresponding to residues 7–16 of the Aα chain of human fibrinogen, Biochemistry 28 (1989) 3094–3105.
[41] A. Henschen, F. Lottspeich, M. Kehl, C. Southan, Covalent structure of fibrinogen, Ann. N.Y. Acad. Sci. 408 (1983) 28–43.
[42] F. Ni, Y. Konishi, L.D. Bullock, M.N. Rivetna, H.A. Scheraga, High-resolution NMR studies of fibrinogen-like peptides in solution: structural basis for the bleeding disorder caused by a single mutation of Gly(12) to Val(12) in the Aα chain of human fibrinogen Rouen, Biochemistry 28 (1989) 3106–3119.
[43] F. Markwardt, Hirudin as an inhibitor of thrombin, Methods Enzymol. 19 (1970) 924–932.
[44] D.K. Sukumaran, G.M. Clore, A. Preuss, J. Zarbock, A.M. Gronenborn, Proton nuclear magnetic resonance study of hirudin: resonance assignment and secondary structure, Biochemistry 26 (1987) 333–338.
[45] H. Haruyama, K. Wüthrich, Conformation of recombinant desulfatohirudin in aqueous solution determined by nuclear magnetic resonance, Biochemistry 28 (1989) 4301–4312.
[46] J.-Y. Chang, The functional domain of hirudin, a thrombin-specific inhibitor, FEBS Lett. 164 (1983) 307–313.
[47] F. Ni, Y. Konishi, H.A. Scheraga, Thrombin-bound conformation of the C-terminal fragments of hirudin determined by transferred nuclear Overhauser effects, Biochemistry 29 (1990) 4479–4489.
[48] T.J. Rydel, K.G. Ravichandran, A. Tulinsky, W. Bode, R. Huber, C. Roitsch, J.W. Fenton II, The structure of a complex of recombinant hirudin and human α-thrombin, Science 249 (1990) 277–280.
[49] Z. Vali, H.A. Scheraga, Localization of the binding site on fibrin for the secondary binding site of thrombin, Biochemistry 27 (1988) 1956–1963.
[50] M.G. Grütter, J.P. Priestle, J. Rahuel, H. Grossenbacher, W. Bode, J. Hofsteenge, S.R. Stone, Crystal structure of the thrombin–hirudin complex: a novel mode of serine protease inhibition, EMBO J. 9 (1990) 2361–2365.
[51] I. Pechik, J. Madrazo, M.W. Mosesson, I. Hernandez, G.L. Gilliland, L. Medved, Crystal structure of the complex between thrombin and the central "E" region of fibrin, Proc. Natl. Acad. Sci. U. S. A. 101 (2004) 2718–2723.
[52] T.H. Donnelly, M. Laskowski Jr., N. Notley, H.A. Scheraga, Equilibria in the fibrinogen–fibrin conversion: II. Reversibility of the polymerization steps, Arch. Biochem. Biophys. 56 (1955) 369–387.
[53] J.D. Ferry, S. Katz, I. Tinoco Jr., Some aspects of the polymerization of fibrinogen, J. Polym. Sci. 12 (1954) 509–516.
[54] W. Krakow, G.F. Endres, B.M. Siegel, H.A. Scheraga, An electron microscopic investigation of the polymerization of bovine fibrin monomer, J. Mol. Biol. 71 (1972) 95–103.
[55] J.M. Sturtevant, M. Laskowski Jr., T.H. Donnelly, H.A. Scheraga, Equilibria in the fibrinogen–fibrin conversion: III. Heats of polymerization and clotting of fibrin monomer, J. Am. Chem. Soc. 77 (1955) 6168–6172.
[56] G.F. Endres, S. Ehrenpreis, H.A. Scheraga, Equilibria in the fibrinogen–fibrin conversion: VI. Ionization changes in the reversible polymerization of fibrin monomer, Biochemistry 5 (1966) 1561–1567.
[57] G.F. Endres, H.A. Scheraga, Equilibria in the fibrinogen–fibrin conversion: VII. On the mechanism of the reversible polymerization of fibrin monomer, Biochemistry 5 (1966) 1568–1577.
[58] W. Kauzmann, Some factors in the interpretation of protein denaturation, Adv. Protein Chem. 14 (1959) 1–63.
[59] G. Némethy, H.A. Scheraga, The structure of water and hydrophobic bonding in proteins: III. The thermodynamic properties of hydrophobic bonds in proteins, J. Phys. Chem. 66 (1962) 1773–1789.

[60] H.A. Scheraga, Theory of hydrophobic interactions, J. Biomol. Struct. Dyn. 16 (1998) 447–460.
[61] G. Némethy, I.Z. Steinberg, H.A. Scheraga, The influence of water structure and of hydrophobic interactions on the strength of side-chain hydrogen bonds in proteins, Biopolymers 1 (1963) 43–69.
[62] A. Fernández, H.A. Scheraga, Insufficiently dehydrated hydrogen bonds as determinants for protein interactions, Proc. Natl. Acad. Sci. U. S. A 100 (2003) 113–118.
[63] A. Shimizu, Y. Saito, Y. Inada, Distinctive role of histidine-16 of the Bβ chain of fibrinogen in the end-to-end association of fibrin, Proc. Natl. Acad. Sci., U. S. A 83 (1986) 591–593.
[64] K. Laki, R. Steiner, Polymerization of iodinated fibrinogen, J. Polym. Sci. 8 (1952) 457–465.